

# SERNet-Former: Semantic Segmentation by Efficient Residual Network with Attention-Boosting Gates and Attention-Fusion Networks

Serdar Erişen  
IEEE, Professional Member  
Ankara, Turkey  
serdarerisen@ieee.org

## Abstract

*Improving the efficiency of state-of-the-art methods in semantic segmentation requires overcoming the increasing computational cost as well as issues such as fusing semantic information from global and local contexts. Based on the recent success and problems that convolutional neural networks (CNNs) encounter in semantic segmentation, this research proposes an encoder-decoder architecture with a unique 'efficient residual network'. Attention-boosting gates (AbGs) and attention-boosting modules (AbMs) are deployed by aiming to fuse the feature-based semantic information with the global context of the efficient residual network in the encoder. Respectively, the decoder network is developed with the additional attention-fusion networks (AfNs) inspired by AbM. AfNs are designed to improve the efficiency in the one-to-one conversion of the semantic information by deploying additional convolution layers in the decoder part. Our network is tested on the challenging CamVid and Cityscapes datasets, and the proposed methods reveal significant improvements on the existing baselines, such as ResNet-50. To the best of our knowledge, the developed network, SERNet-Former, achieves state-of-the-art results (84.62 % mean IoU) on CamVid dataset and challenging results (87.35 % mean IoU) on Cityscapes validation dataset.*

## 1. Introduction

Semantic segmentation is a fundamental computational task that is widely applied in 2D scene understanding in the research field of computer vision. In semantic segmentation, each pixel is mapped through the labeled semantic classes, introduced via the ground truth of an image input, that is tried to be predicted by state-of-the-art networks and methods. Among the number of benefits of semantic segmentation, autonomous driving, and robotics in recognizing indoor and outdoor scenes, medical imaging, virtual reality, augmented reality, real-time surveillance, scene understanding, photography, creating, and editing images [1-3] can be counted as the widely used

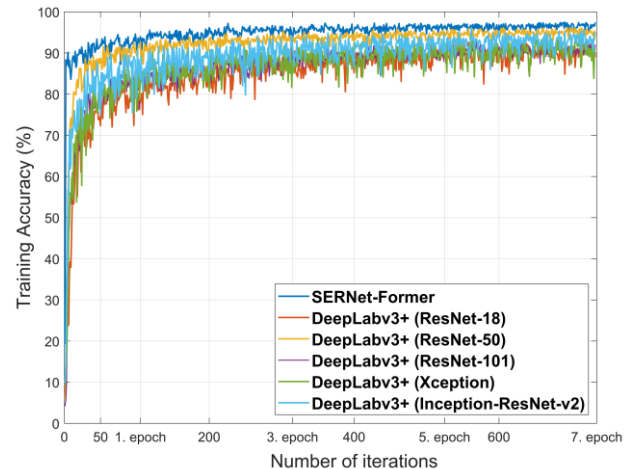


Figure 1. Training progress of SERNet-Former and the selected baselines of DeepLabv3+ on CamVid dataset. (Viewed best in color)

applications and emerging research fields. Many different types of deep neural networks (DNNs), including Fully Connected Network (FCN) and Convolutional Neural Networks (CNNs), applying encoder-decoder architectures and attention-based models, have shown remarkable progress [2-4]. Recently, Vision Transformers (ViT) with Swin Transformers [5-8] and CNN architectures achieved state-of-the-art performances in semantic segmentation [2, 4].

Fusing the multi-scale semantic information is one of the compelling issues in segmentation tasks besides the concerns of computational cost and efficiency of the developed networks and methods. The challenge of recognizing objects in semantic segmentation in 2D scenes is two-fold: The labeled object may either lose its spatial information or feature-rich properties during the processing of the image throughout the network. Most recent state-of-the-art networks [2, 4, 9] also try to overcome the inconsistency between the semantic information from the global and local contexts of a given image input. Thus, the spatial information and feature maps in CNNs are aimed to be discovered deeply for efficient and precise semantic segmentation in this work.

It is another intriguing fact that increasing the number of convolution layers does not always return efficient results when compared to its computational cost [10], such as using Inception-ResNet-v2 as the baseline architecture without enlarging its decoder part (Fig. 1). In that regard, rather than using the largest CNNs, the research dives into the deep potential of the improved performance of CNNs with additional methods. This work re-evaluates the efficiency of the CNN-based encoder-decoder architectures with attention-based fusion networks and modules. The study discovers the potential of fused attention gates, not only used in the head of the developed network architectures but also fused within the decoder.

Therefore, it is first explored to find the most efficient baseline architecture that can be trained fast and should be lightweight (Fig. 1). In this research, ResNet-50 [11] is analyzed as the baseline for further improvement on the head of the encoder network. Different types of attention gates are developed together with convolution layers in the encoder and decoder parts. The role of spatial information, fused with channel-based semantic information, is also discovered by carefully placing the skip connections at the right steps in the encoder and decoder networks.

Thus, the encoder of our network is improved with the attention-boosting gates (AbGs), resulting in an ‘efficient residual network’ with increased training performance and prediction efficiency. Notwithstanding this, larger networks can perform far better than the shallower networks in longer training periods. In that regard, attention-fusion networks (AfNs) are deployed as another method, adapted to the decoder part of our network, to improve its capacity by storing, fusing, and processing rich semantic information from the encoder during up-sampling. Thus, attention-fusion networks are designed to superpose the global spatial context with feature-based rich semantic information to improve the performance of CNNs with fewer layers. Our methods show significant improvements in the trained baseline architectures in the initial epochs on CamVid dataset [12-13]. Fig. 1 illustrates the comparison of the initial training performance of some networks using CNNs as the baseline architectures. Respectively, SERNet-Former learns much faster than the quickest learning baseline, ResNet-50, that is applied in DeepLabv3+ architecture [9, 14] during training sessions on CamVid dataset.

In brief, our network is developed from the residual CNNs by adding attention-boosting gates and attention-fusion networks. Our additional methods are connected to the encoder and decoder parts via skip connections to fuse the rich information of feature maps from different contexts, concatenated by superposing the useful semantic information for the highest efficiency. To the best of our knowledge, an ‘efficient residual network’ is developed that is unique in the literature used as the head and encoder of our network. The network is improved by attention-

boosting gates and attention-fusion networks with increasing efficiency and precision in predicting and recognizing smaller objects and their features. As being highly inspired by RGB-D networks [15-16], the methods of attention-based fusion modules and networks are also deployed with an aim to adapt our model for different classification tasks and feature maps of RGB-D inputs and 3D point clouds for future work. Our contributions can be briefly highlighted as follows:

- A unique ‘efficient residual network’ is developed as an encoder with the additional excitation by attention-boosting gates (AbGs) with a search for the optimal training performance and computational cost of CNNs
- The capacity of the decoder part of our network is improved via attention-fusion networks (AfNs), increasing the efficiency of acquiring and processing the feature-rich semantic information
- Skip connections, turning the decoder part into a superposition network, are designed to fuse and concatenate multi-scale information from the global and local contexts
- The network achieves state-of-the-art performances on CamVid and Cityscapes *validation* datasets.

## 2. Related Works

The multi-scale problem in semantic segmentation can also be described as the discrepancy in integrating rich spatial and channel-based semantic information of an object acquired from the global and local contexts of a network. DeepLabv3+ [9] also depends on fusing feature-based rich semantic information with the spatial information of objects in 2D scenes, just as in other encoder-decoder networks like U-Net and Segnet [17-18]. Thus, Chen et al. [9] studied various down-sampling and up-sampling options for efficient semantic information processing and fast training and learning progress. They also experimented with the modifications of baselines, such as Xception and ResNet-101, to improve the efficiency of DeepLabv3+ [9]. The recent success of convolutional neural networks with the potential of dynamic weights and long-range dependencies [2, 4] also revealed that CNNs could be developed with additional methods, such as transform gates using the Sigmoid function [19], as well as ViTs for multi-scale representations, which become the choice for the extra-large scale networks [20].

Fusing the global and local semantic information in encoder-decoder architectures can become challenging due to the loss of semantic features during down-sampling and up-sampling [21-22]. Li et al. [22] introduced global enhancement and local refinement methods that are

integrated through a Context Fusion Block. Similarly, Guided Attention Inference Network (GAIN) [21] uses fully convolutional networks and CNN-based semantic segmentation architectures, such as DeepLab [9, 14], with commonly used baseline architectures, like ResNet-101 [11, 23].

Squeeze-and-Excitation block, SENet [24], has also been introduced to improve the dependencies between the global and local semantic information and spatial and channel-wise features. Similarly, self-attention mechanisms are developed to acquire feature-rich information of objects at each position by aggregating features from all locations in a single sample [25]. Accordingly, Guo et al. [25] proposed external attention module using memory units by replacing the self-attention mechanisms in semantic segmentation networks. The inspirations from SENet and self-attention mechanisms also motivated SAB Net with an end-to-end semantic attention-boosting framework [26]. The applied method proposes a nonlocal semantic attention framework, which regularizes the difference between the nonlocal and local information by applying a category-wise learning weight [26]. CTNet has another alternative approach, utilizing two modules: Channel Contextual Module, for exploring the multi-scale local channel contexts, and Spatial Contextual Module, for exploring the global spatial dependency, in a tandem configuration [27].

In integrating the transformer architectures with self-attention mechanisms, CoTNet was developed with Contextual Transformer Block, which enables transforming and replacing each discrete convolutional operator, such as  $3 \times 3$  convolution, with two consecutive  $1 \times 1$  convolutions [28]. Alternatively, Ye et al. [29] introduced cross-modal self-attention that was proposed to integrate the image and language expressions as inputs as a result of the rising success of ViTs.

Attention-based feature fusion has also emerged as another solution to the challenging multi-scale problem in semantic segmentation [30]. Across feature map is used as an alternative method in dealing with small objects, which are hard to determine with their semantic features and exact location information [31]. Differently, Choe et al. [32] proposed the attention-based dropout layer, which hides the most discriminative parts from the model by utilizing a drop mask and importance map while keeping the classification accuracy.

As another alternative to attention-fusion networks, the covariance attention method was proposed by Liu et al. [33], such that the covariance matrix maps the dependency between local and global semantic features. Similarly, the variational structured attention mechanism was proposed by Yang et al. [34] to integrate channel-based and spatial features. According to their method, the structured attention mechanism produces the tensor products of spatial attention and channel-wise attention modules and

enables the evaluation of the probabilities of latent variables that are mapped between the channel-wise and spatial attention mechanisms [34]. Hao et al. [35] proposed spatial-detail-guided context propagation by aiming to reconstruct the lost information in low-resolution global contexts using the spatial details of shallower layers in real time. Huang et al. [3] proposed CCNet as a crisscross attention network and a novel alternative to self-attention networks and attention mechanisms.

The integration of spatial information and channel-based rich semantic features is also analyzed by various novel research dealing with RGB-D networks and 3D point clouds, such as ShapeConv, S-Conv, PointMTL, and MLFNet [36-39]. Respectively, this research evaluates the potential of CNN with attention-based mechanisms and explores the potential and limits of resilient baseline architectures for different tasks including 2D and 2.5D semantic segmentation.

### 3. Methodology

In this research it is aimed to develop an encoder-decoder architecture with additional methods to improve the performance of the network by regarding the problem of fusing semantic information from different contexts. In the exploration of efficient head network to be improved for fast and accurate training without losing the existing progress of baseline architectures, attention-boosting gates (AbGs) and attention-boosting modules (AbMs) are designed to excite and fuse the feature-rich spatial information into the existing networks. It is found that in the short run, ResNet-50, pre-trained on ImageNet dataset, can be the most efficient and fastest residual network (Fig. 1) to be improved in learning most of the features in a few epochs even if it can have the capacity problems for more new features. Respectively, our head network is advanced by introducing attention-boosting gates to the selected baseline, as they efficiently increase the probability of exciting semantic information in producing feature maps. AbGs are fused with the spatial context of the head by attention-boosting modules, which result in a novel ‘efficient residual network’ that is used as the encoder part of our network. To provide an efficient transition between the encoder and decoder networks of the developed architecture, dilation-based convolution layers are used.

Prediction in semantic segmentation needs to decrease the loss during training, which is directly related to the applied loss function as well as the one-to-one conversion of the acquired data from the encoder network, transferred to the classification layer. Thus, it is also related to the efficiency of decoding the semantic information. Inspired by AbG, attention-fusion networks (AfNs) are designed to increase the efficiency in signal processing in the decoder part of our network by fusing the feature-rich semantic information from the encoder. In overcoming the capacity

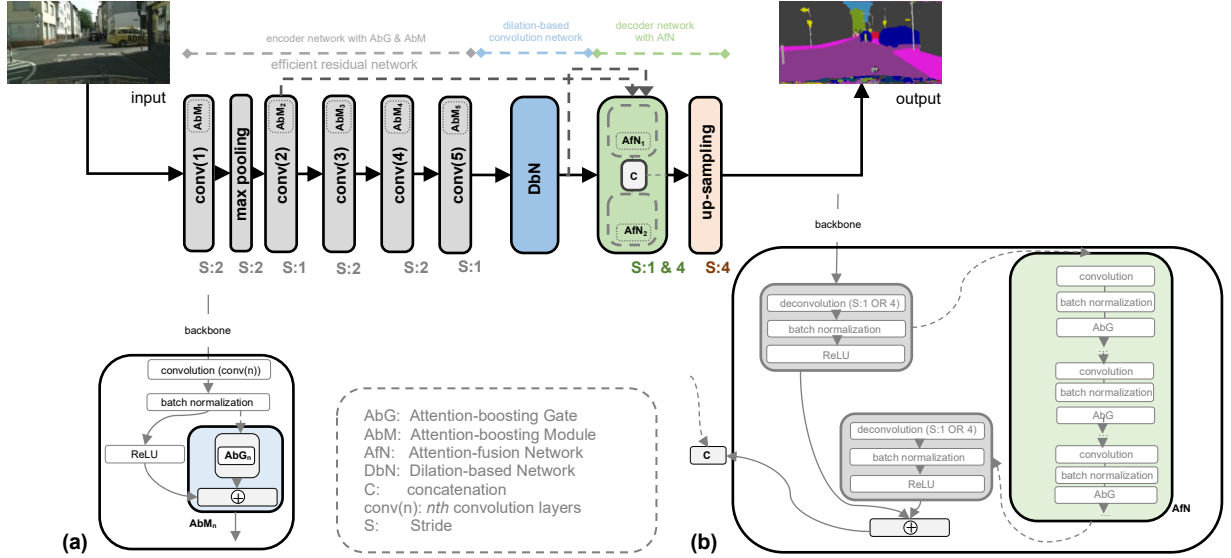


Figure 2. Schematic illustration of SERNet-Former. (a) Attention-boosting Gate (AbG) and Attention-boosting Module (AbM) are fused into the encoder part. (b) Attention-fusion Network (AfN), introduced into the decoder. (Viewed best in color)

problems of smaller and medium residual networks, convolution layers are also used in attention-fusion networks. Respectively, skip connections are designed to have the most efficient results for fusing multi-scale feature maps in the decoder part of our network.

Finally, the loss function and pixel classification layer of our network are set with regard to the commonly applied evaluation methods in the literature and the class weights of each class in the experiment datasets. The methods applied in improving the efficiency of our network can be briefly denoted as follows:

- An efficient residual network is developed as the encoder part of our network with AbGs and AbMs
- Dilation-based convolution network is introduced between the encoder and decoder parts
- Decoder part of our network is improved by AfNs with the help of skip connections
- Loss function and pixel classification layer are optimized with regard to the applied evaluation methods and datasets.

### 3.1. The efficient residual network head: Encoder with attention-boosting modules

Attention-boosting gate aims to excite channel-wise rich semantic information that may not be filtered through ReLU layers. The output of the Sigmoid function can increase the possibility of producing and evaluating feature maps that may not be activated through residual networks. In that regard, the Sigmoid function, which is widely

applied in attention networks, is selected as the operator to increase the possibility of acquiring and processing channel-wise and feature-based rich semantic information that could not be activated in the commonly used baseline architectures. The operation of the gate, AbG, can be iterated in Equation (1) as follows:

$$AbG_n = Sigmoid(i_{BN(conv)_n}) \times (i_{BN(conv)_n}), \quad (1)$$

where  $i_{BN(conv)_n}$  denotes the output of the  $n$ th convolution and the following batch normalization layers and Equation (1) defines a multiplication function. AbG returns the rich feature maps by the product of the probability of the acquired features of channel-based semantic information with the outcome of the convolution layers. Accordingly, attention-boosting module, AbM, fuses the acquired and processed feature-based semantic information with the spatial context of the residual networks, as illustrated in Fig. 2 (a). The product is fused by element-wise addition into the residual network together with the filtered output of the convolution layers. As a result of introducing the attention-boosting gates into the encoder, the semantic information processed in the head network is changed, and a novel ‘efficient residual network’ architecture is developed (Fig. 2).

AbMs are added to the baseline at the end of each  $n$ th convolution layer. It works as a mathematical operator for exciting and fusing the feature-rich semantic information. It can also be introduced into different networks to acquire and process feature maps from 3D point clouds or RGB-D networks for different tasks.

### 3.2. Dilation-based separable convolution network

Dilation-based convolution network (DbN) is applied to

increase the probability of searching, recognizing, and comparing the local, channel-based, and rich semantic information between the encoder and decoder parts by decomposing the output into smaller feature maps [9] (Fig. 2). Thus, the output of the encoder architecture is moved into convolutional layers, with 12, 16 and 18 dilation factors, together with the following batch normalization and ReLU layers, and they are fused together before the decoder network.

### 3.3. Decoder with attention-fusion networks

Inspired by the methods used for AbG and AbM, the efficiency of fusing global and local contexts into the decoder part of the network is improved by attention-fusion networks. Even though the initial layers of CNNs are rich in the global context of semantic information with sharp edges and apparent shapes of objects, it is very significant to transfer and reconstruct that semantic information during the up-sampling tasks in the decoder part of the network for efficient one-to-one image processing.

Thus, AfNs are introduced into the decoder network for processing and fusing the semantic information with the global and local contexts from the encoder part. It is also aimed to increase the capacity of storing semantic information in the decoder part of the network regarding the limitations of smaller and simpler residual networks. Respectively, AfNs are designed and fused with convolution layers, as illustrated in Fig. 2 (b). The spatial and channel-based contextual semantic information from deconvolution layers with different strides are gathered by the concatenation of the products of AfNs via the depth concatenation layer (Fig. 2). In that regard, skip connections are used to increase the efficiency of the network in acquiring the spatial information from the encoder, concatenated with the channel-based features during the up-sampling operations.

### 3.4. Loss function and the classification layer

For calculating the classification performance of our semantic segmentation network, cross-entropy loss function is deployed via the pixel classification layer, as in Equation (2).

$$loss = - \sum_{x \in classes}^c T(x) \times \log Y(x), \quad (2)$$

where  $T$  denotes the target,  $x$  is a class in the labeled classes  $C$  in a dataset. Thus,  $Y$  stands for the predicted pixels. Before the experiments, the pixel classification layer is executed by calculating the class weights for each labeled class in each dataset separately. Then, crossentropy function is deployed to use Equation (2) in calculating the loss between the prediction of the network and the ground truth.

### 3.5. Evaluation metrics

In the evaluation of the semantic segmentation tasks, pixel accuracy ( $pa$ ) is calculated as the ratio of correct prediction of pixel over the total number of pixels with  $N$  number of classification labels and the background as in Equation (3).

$$pa = \frac{\sum_{i=0}^N p_{ii}}{\sum_{i=0}^N \sum_{j=0}^N p_{ij}}, \quad (3)$$

where  $p_{ii}$  stands for the number of pixels that are predicted as the classification label  $i$ , whereas  $p_{ij}$  is the ground truth that also includes the number of pixels that belong to other labels  $j$ . In that regard, the mean pixel accuracy is calculated by Equation (4).

$$mean(pa) = \frac{1}{(N + 1)} \times \frac{\sum_{i=0}^N p_{ii}}{\sum_{i=0}^N \sum_{j=0}^N p_{ij}}. \quad (4)$$

Moreover, the exact performance in segmentation tasks is calculated by the Intersection over Union ( $IoU$ ) method deploying the *Jaccard* index as in Equation (5).

$$IoU = \frac{|A \cap B|}{|A \cup B|}, \quad (5)$$

where  $A$  is the predicted segmentation map, and  $B$  stands for the ground truth. Thus, mean  $IoU$  ( $m(IoU)$ ) is calculated by the average  $IoU$  over all classes [1].

## 4. Experiments and Results

In this section, the experiment datasets and the implementation details are introduced first. The results for each open-source dataset are analyzed to be compared with other state-of-the-art networks in the literature by discussing the influence of the methods applied to develop our network. Accordingly, ablation studies are conducted to analyze the contribution of each method.

### 4.1. Datasets

**The Cambridge-driving Labelled Video Database (CamVid)** [12-13] is one of the first scene understanding databases, and it is based on the motion-based video collections of driving scenes recorded for semantic segmentation of object classes. This database contains 701 frames with sizes of 720×960 pixels that were captured in five video sequences, shot via the fixed-position CCTV-style cameras mounted on a car. The densely annotated images were manually generated through 32 classes and merged into 11 classes later. The original dataset is divided into 367 training, 101 validation, and 233 test images, as most literature practiced.

**Cityscapes** [40] is one of the most challenging datasets for the semantic segmentation of urban street scenes. It contains high-quality pixel-level annotations for 5000 images, as well as coarsely annotated 20000 images. The

Table 1. Class accuracies (mIoU) of state-of-the-art methods on CamVid dataset

Method	Building	Tree	Sky	Car	Sign	Road	Pedestrian	Fence	Pole	Sidewalk	Bicycle	mIoU
Dilation8 [41]	82.6	76.2	89	84	46.9	92.2	56.3	35.8	23.4	75.3	55.5	65.3
BiSeNet [42]	83	75.8	92	83.7	46.5	94.6	58.8	53.6	31.9	81.4	54	68.7
VideoGCRF [43]	86.1	78.3	91.2	92.2	63.7	96.4	67.3	63	34.4	87.8	66.4	75.2
DeepLabv3Plus+SDCNetAug (SS) [44]	90.9	82.9	92.8	94.2	69.9	97.7	76.2	74.7	51	91.1	78	81.7
DeepLabv3Plus+SDCNetAug (MS) [44]	91.2	83.4	93.1	93.9	71.5	97.7	79.2	76.8	54.7	91.3	79.7	82.9
<b>SERNet-Former (ours)</b>	<b>93</b>	<b>88.8</b>	<b>95.1</b>	91.9	<b>73.9</b>	97.7	76.4	<b>83.4</b>	<b>57.3</b>	90.3	<b>83.1</b>	<b>84.62</b>

dataset contains diverse stereo video sequences with the sizes of  $1024 \times 2048$  pixels, recorded during the daytime of 50 European cities visited in several months (spring, summer, and fall) with good or average weather conditions [40]. The dataset of 5000 fine annotations is divided into three sets: 2975 for training, 500 for validation, and 1525 for testing. The dataset includes semantic, instance-wise, and dense pixel annotations of 30 classes grouped into eight categories. However, most literature uses annotations with 20 classes, 19 of which are semantic labels containing objects and stuff, in addition to one additional void class for do-not-care regions.

## 4.2. Implementation details and experiment results

In the experiments on CamVid dataset, 11 classified categories are used. During the training, the images are kept to their original sizes of 720 by 960 pixels. Thus, only the single scale (SS) method is used in training and testing the dataset. The dataset split is kept similar to the commonly applied option in the literature. Respectively, the mini-batch size is set to 3, the initial learning rate is set to  $1e^{-3}$ , and our network is trained for 80 epochs. The network is trained and tested on the arranged CamVid test dataset in MATLAB. Per-class *mIoU* results with regard to the classified categories are reported in Table 1. The experiment results of our network, compared with well-known state-of-the-art models, are reported in Table 2.

In overcoming the imbalanced number of instances among different categories, the weighted scores for each class in CamVid and Cityscapes datasets are analyzed first. Accordingly, the weight values are assigned in the pixel classification layer. Stochastic gradient descent with momentum (SGDM) optimizer is used as the optimization algorithm during all training sessions for both datasets. Different L2Regularization values are used throughout the training schedule to decrease losses and increase the efficiency of our network on both datasets. For both datasets, the multi-scale (MS) method is not deployed. The hardware resource of Intel® Core™ i5-6200 CPU at 2.30–2.40 GHz with 16 GB memory is used for all experiments.

Table 2. Test results on CamVid dataset

Method	mIoU	SS/ MS	Baseline Architecture	Params (M)
Dilation8 [41]	65.3	MS	VGG-16	-
BiSeNet [42]	68.7	SS	ResNet-18	49.0
VideoGCRF [43]	75.2	SS	ResNet-101	-
CCNet [3]	79.1	SS	ResNet-101	-
DeepLabv3+SDCNet Aug [44]	81.7	SS	WideResNet38	-
DeepLabv3+SDCNet Aug [44]	82.9	MS	WideResNet38	-
RTFormer-Slim [45]	81.4	SS	-	4.8
RTFormer-Base [45]	82.5	SS	-	16.8
SIW (SegFormer B5) [6, 46]	83.7	SS	MiT-B5 (IM-1K, MV)	84.7
<b>SERNet-Former (ours)</b>	<b>84.62</b>	SS	<b>SERNet-Former</b>	44.2

Minibatch size is set to 1 during training on Cityscapes datasets to test the network for real-world scenarios with limited hardware resources. The images from the *leftImg8bit* dataset are trained with *instanceIDs* with fine annotations, and the initial learn rate is set to  $5e^{-4}$ . To overcome the long period of training processes, efficient self-training methods [47], by selecting the samples from the dataset for faster training, are deployed in the experiments. The network is initially trained through the selected 715 samples with 20 classes, including the background. Then, the developed network is further trained with 19 classes, including all samples. Thus, the network, pre-trained on CamVid dataset, is trained for 80 epochs in MATLAB for the performance evaluation. During training, the images are kept to their original sizes of 1024 by 2048 pixels. Per-class *mIoU* results on Cityscapes are reported in Table 3. The experiment results of our network on Cityscapes datasets are reported in Table 4, together with the results of well-known state-of-the-art methods.

## 4.3. Comparison with regard to state-of-the-art

During the experiments on CamVid dataset, different baselines of DeepLabv3+, such as ResNet-18, ResNet-50, ResNet-101, Xception, and Inception-ResNet-v2, are trained in MATLAB and compared with the results of our network (Fig. 1). Accordingly, ResNet-50 is found efficient, due to its size and learning progress, to be modified and improved further as our encoder.

Table 3. Per-class accuracies (mIoU) based on Cityscapes datasets

Method	dataset	flat		construction			object			nature		sky	person		vehicle					mIoU	
		road	sidewalk	building	wall	fence	pole	traffic light	traffic sign	vegetation	terrain	sky	person	rider	car	truck	bus	train	motorcycle		bicycle
Dilation10 [41]	test	97.6	79.2	89.9	37.3	47.6	53.2	58.6	65.2	91.8	69.4	93.7	78.9	55	93.3	45.5	53.4	47.7	52.2	66	67.1
PSPNet+ [48]	test	98.7	86.9	93.5	58.4	63.7	67.7	76.1	80.5	93.6	72.2	95.3	86.6	71.9	96.2	77.7	91.5	83.6	70.8	77.5	81.2
Gated-SCNN [49]	test	98.7	87.4	94.2	61.9	64.6	72.9	79.6	82.5	94.3	74.3	96.2	88.3	74.2	96.0	77.2	90.1	87.7	72.6	79.4	82.8
HANet++ [50]	test	98.8	88.0	94.2	66.6	64.8	72.0	78.2	81.4	94.2	74.5	96.1	88.1	75.6	96.5	80.3	93.2	86.6	72.5	78.7	83.2
DeepLabv3 [14]	test	98.6	86.2	93.5	55.2	63.2	70.0	77.1	81.3	93.8	72.3	95.8	87.6	73.4	96.3	75.1	90.4	85.1	72.1	78.3	81.3
DeepLabv3+ [9]	test	98.7	87	93.9	59.5	63.7	71.4	78.2	82.2	94	73	95.8	88	73	96.4	78	90.9	83.9	73.8	78.9	82.1
DPC [51]	test	98.7	87.1	93.8	57.7	63.5	71.0	78.0	82.1	94.0	73.3	95.4	88.2	74.5	96.5	81.2	93.3	89.0	74.1	79.0	82.7
Zhu et al. [44]	test	98.8	87.8	94.2	64.1	65	72.4	79	82.8	94.2	74	96.1	88.2	75.4	96.5	78.8	94	91.6	73.8	79	83.5
Panoptic DeepLab [52]	test	98.8	88.1	94.5	68.1	68.1	74.5	80.5	83.5	94.2	74.4	96.1	89.2	77.1	96.5	78.9	91.8	89.1	76.4	79.3	84.2
Chen et al. [53]	test	98.7	87.3	93.9	63.8	62.7	70.8	77.9	82.2	93.9	72.8	95.9	88.2	75.2	96.5	80.4	91.6	89	73.2	78.9	82.8
HRNet+OCR ASPP [54]	test	98.8	88.3	94.3	66.9	66.7	73.3	80.2	83	94.2	74.1	96	88.5	75.8	96.5	78.5	91.8	90.1	73.4	79.3	83.7
iFLYTEK-CV [55]	test	98.8	88.4	94.4	68.9	68.9	73	79.7	83.3	94.3	74.3	96	88.8	76.3	96.6	84	94.3	91.7	74.7	79.3	84.4
Tao et al. [55]	test	99	89.2	94.9	71.6	71.6	75.8	82	85.2	94.5	75	96.3	90	79.4	96.9	79.8	94	85.8	77.4	81.4	85.1
<b>SERNet-Former*</b> (ours)	test	97.0	76.4	89.5	46.5	47.9	55.0	63.0	69.0	91.3	67.1	94.0	79.7	61.3	93.1	50.8	62.4	54.2	57.8	67.3	69.65
<b>SERNet-Former**</b> (ours)	test	96.8	76.3	90.0	57.2	54.6	52.9	60.5	66.0	90.9	64.6	93.9	79.0	61.6	93.5	69.7	85.3	74.7	59.7	65.6	73.31
<b>SERNet-Former†</b> (ours)	test	98.2	<b>90.2</b>	94.0	67.6	68.2	73.6	78.2	82.1	94.6	75.9	<b>96.9</b>	<b>90.0</b>	77.7	<b>96.9</b>	<b>86.1</b>	93.9	<b>91.7</b>	70.0	<b>82.9</b>	84.83

\*: ResNet-50 without AbM, DbN, AfN, trained 60 epochs. \*\*: ResNet-50 without AbM, DbN, AfN. †: with AbM, DbN, AfN, trained 60 epochs

Table 4. Results of state-of-the-art methods on Cityscapes datasets

Method	Baseline Architecture	mIoU test Dataset	Params (M)	mIoU validation Dataset
ResNet-38 [10]	ResNet-38 (A2, 2, val.)	81.3	-	77.86
PSPNet++ [48]	ResNet-101	81.2	-	79.7
PSANet+ [56]	ResNet-101	81.4	-	-
CCNet [3]	ResNet-101	81.9	-	80.2
OCR [57]	ResNet-101	81.8	10.5	-
Gated-SCNN [49]	WideResNet	82.8	(+0.13)	80.8
HANet++ [50]	ResNeXt-101	83.2	65.4	80.29
ResNeSt [58]	ResNeSt	83.3	70	82.7
DeepLabv3 [14]	ResNet-101	81.3	-	78.5
DeepLabv3+ [9, 59]	Dilated-Xception-71	82.1	43.48	79.6
Auto-DeepLab [59]	Auto-DeepLab-L	82.1	44.42	80.33
DPC [51]	Xception	82.7	(+0.81)	80.85
kMaX-DeepLab [60]	ConvNeXt-L	83.2	232	83.5
Zhu et al. [44]	WideResNet38	83.5	-	81.4
Panoptic DeepLab [52]	SWideRNet	84.2	46.72	83.1
AdapNet++ [61]	ResNet-50	81.34	30.2	81.24
SSMA [61]	ResNet-50	82.31	56.44	82.19
EfficientPS [62]	EfficientNet-B5	84.21	-	82.1
SegFormer [6]	MIT-B5(IM-1K, MV)	83.7	84.7	84.0
Lawin+ [20]	Swin-L (IM-22K)	84.4	201.2	-
ViT-Adapter-L [8]	ViT-Adapter-L	85.2	347.9	-
HRNetV2+OCR [54]	HRNetV2-W48	83.7	-	86.3
HRNetV2+OCR+PSA [54]	HRNetV2-W48	84.5	-	86.95
Tao et al. [55]	HRNet-OCR	85.1	-	-
HS3-Fuse [2]	HRNet48-OCR-HMS	85.7	-	-
HS3-Fuse [2]	HRNetV2-W18	-	-	81.8
InternImage-H [4]	InternImage (T)	86.1	1080	87.0
<b>SERNet-Former</b> (ours)	SERNet-Former	84.83 <sup>†</sup>	44.2	<b>87.35</b>

†: trained 60 epochs

It is apparent from the results that even if MS method is not deployed, our network returns state-of-the-art results on CamVid dataset, with the help of a novel ‘efficient residual network’ and the decoder, improved with AfNs (Tables 1 and 2). The announced accuracies for each class reveal the efficiency of our network with the applied methods when compared to the other networks, especially in recognizing the tiny objects that have less pixel area on the canvas, such as poles or bicycles, and occluding objects, such as trees and fences that can be confused with other classes, such as buildings (Table 1). When compared to other methods, our network has also performed better with regard to its size and the number of parameters it uses as illustrated in Table 2. The results also reveal that AbM and AfN decrease the loss in the initial training epochs

successfully, increasing the actual test performance and accuracy of the segmentation network.

Based on the results on Cityscapes validation and *test* datasets, our network is successful in recognizing the objects far from the ego-vehicle (Fig. 3), and especially in identifying the classes such as sidewalk, sky, person, car, truck, train, and bicycle (Table 3). When considering its size and the number of parameters that are used, our network indeed performs much better than most of the state-of-the-art methods with the incomparable number of parameters, and it puts forth challenging performance results on Cityscapes *validation* dataset (Table 4).

On the other hand, most of the announced results of other state-of-the-art models and methods on Cityscapes datasets apply multi-scale (MS) crop sizes as well as additional, coarse datasets. In that regard, even though the results for each classified label show the considerable performance of our network, it is still hard to have a fair comparison with other state-of-the-art methods based on the results for Cityscapes datasets. Moreover, image comparisons reveal that our model can sometimes fail in predicting very sharp geometric forms that the ground truth claims even though the real-world scene also appears similar to the predicted (Fig. 3), which is also left to be analyzed further.

#### 4.4. Ablation Studies

Ablation studies are performed on CamVid dataset during the development progress of the network. Since modules such as AbM and AfN are fused by element-wise additions, ablation studies could be done by removing the added methods and by getting the final validation of the trained network (Table 5). For assessing the influence of the dilation-based network, however, a simpler network without the dilation-based convolution layers is used instead of DbN in ablation studies, and the results are reported in Table 5.

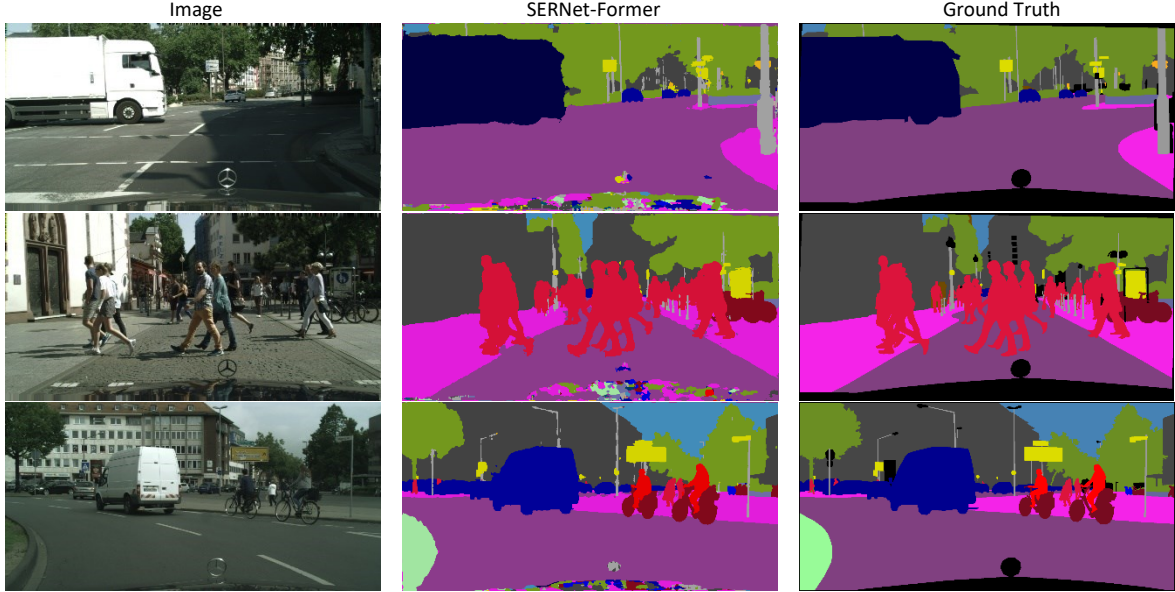


Figure 3. Examples from the test results on Cityscapes *validation* dataset. (Viewed best in color)

AbM is designed to be introduced or removed easily to the baseline architectures. However, removing AbM from the initial convolution layers of residual networks can completely change the outcomes of the network. In that regard, the efficiency of AbM can be observed best at the end of the last convolution layer of the encoder.

According to the ablation studies, the attention-boosting module (AbM<sub>5</sub>), added to the last convolution layer of the head network, augments the feature-based and channel-wise contextual semantic information of the network, and increases its efficiency by 1.656 percent (Table 5). Thus, each AbM can have a share of 1.99 percent in the improvement of the network theoretically. Accordingly, DbN has a 2.79 percent share in the improved performance of the network (Table 5).

Table 5. Ablation studies on CamVid dataset

AbM <sub>5</sub>	AfN <sub>1</sub>	AfN <sub>2</sub>	DbN	mIoU (%)
	✓	✓	✓	81.224 (-1.656) (1.99 %)
✓	✓	✓	✓	80.562 (-2.318) (2.79 %)
✓	✓	✓	✓	78.987 (-3.893) (4.69 %)
✓	✓	✓	✓	75.371 (-7.509) (9 %)
✓	✓	✓	✓	82.88

AfNs are designed to increase the performance of the decoder and decrease the training loss accordingly. The influences of the AfNs, which are introduced with the deconvolution layers with different strides in the decoder part of the network, are seen as extremely significant. When AfN is introduced into the following deconvolution layer with stride 1 (AfN<sub>1</sub>), it adds up to 3.893 percent to the overall test performance and improves the network with a share of 4.69 percent (Table 5). When AfN is fused into the decoder with the following deconvolution layer with stride 4 (AfN<sub>2</sub>), it improves the network’s performance by more

than 7.5 percent. Based on the earlier test results (Table 5), AfN<sub>2</sub> contributes to the improvement of the network by 9 percent as it also processes the spatial information with different sizes and contexts fused into the network.

## 5. Conclusion

Regarding the problem of fusing semantic information from different contexts, a novel and efficient residual network is developed in an encoder-decoder architecture. Attention-boosting gates and attention-fusion networks, in which the Sigmoid function is used to increase the possibility of activating the channel-based feature maps, improve the efficiency of the network with the rising performance by fusing semantic information from the local and global contexts.

Our head network and the encoder part of SERNet-Former are still open to be improved and tested on the challenging datasets for classification tasks. The decoder part of our network can still be improved with AfNs. Respectively, applying our methods on larger residual networks and CNN with more layers by enlarging the decoder part of baseline architectures remains future work. Additional methods that are not applied during experiments, such as multi-scale (MS) crop sizes of images as well as additional coarse datasets that most literature applies, can also improve the results of our network. Moreover, SERNet-Former is developed as having potential for different tasks using feature maps of RGB-D networks and 3D point clouds, and it can be tested for real-time segmentation tasks and real-world applications with limited hardware resources, which also remain as future work.

## References

- [1] S. Minaee, Y. Boykov, F. Porikli, A. Plaza, N. Kehtarnavaz, and D. Terzopoulos. Image Segmentation Using Deep Learning: A Survey. *IEEE Transactions on Pattern Analysis and Machine Intelligence*, 44(7):3523-3542, 2022.
- [2] S. Borse, H. Cai, Y. Zhang, and F. Porikli. HS3: Learning with Proper Task Complexity in Hierarchically Supervised Semantic Segmentation. *arXiv preprint arXiv:2111.02333*, 2021.
- [3] Z. Huang, X. Wang, Y. Wei, L. Huang, H. Shi, W. Liu, and T. Huang. CCNet: Criss-Cross Attention for Semantic Segmentation. *IEEE Transactions on Pattern Analysis and Machine Intelligence*, 45(6):6896-6908, 2023.
- [4] W. Wang, J. Dai, Z. Chen, Z. Huang, Z. Li, X. Zhu, X. Hu, T. Lu, L. Lu, H. Li, X. Wang, and Y. Qiao. InternImage: Exploring Large-Scale Vision Foundation Models with Deformable Convolutions. *arXiv preprint arXiv:2211.05778v3*, 2023.
- [5] H. Du, J. Wang, M. Liu, Y. Wang, and E. Meijering. SwinPA-Net: Swin Transformer-Based Multiscale Feature Pyramid Aggregation Network for Medical Image Segmentation. *IEEE Transactions on Neural Networks and Learning Systems*, 2022.
- [6] E. Xie, W. Wang, Z. Yu, A. Anandkumar, J. M. Alvarez, and P. Luo. SegFormer: Simple and Efficient Design for Semantic Segmentation with Transformers. In *NeurIPS*, 2021.
- [7] Z. Liu, Y. Lin, Y. Cao, H. Hu, Y. Wei, Z. Zhang, S. Lin, and B. Guo. Swin transformer: Hierarchical vision transformer using shifted windows. In *ICCV*, 2021.
- [8] Z. Chen, Y. Duan, W. Wang, J. He, T. Lu, J. Dai, and Y. Qiao. Vision transformer adapter for dense predictions. *arXiv preprint arXiv:2205.08534*, 2022.
- [9] L.-C. Chen, Y. Zhu, G. Papandreou, F. Schroff, and H. Adam. Encoder-Decoder with Atrous Separable Convolution for Semantic Image Segmentation. In *ECCV 2018. Lecture Notes in Computer Science*, Munich, 2018.
- [10] Z. Wu, C. Shen, and A. van den Hengel. Wider or Deeper: Revisiting the ResNet Model for Visual Recognition. *Pattern Recognition*, 90:119-133, 2019.
- [11] K. He, X. Zhang, S. Ren, and J. Sun. Deep residual learning for image recognition. In *CVPR*, pages 770-778, 2016.
- [12] G. J. Brostow, J. Shotton, J. Fauqueur, and R. Cipolla. Segmentation and Recognition Using Structure from Motion Point Clouds. In *ECCV*, 2008.
- [13] G. J. Brostow, J. Fauqueur, and R. Cipolla. Semantic Object Classes in Video: A High-Definition Ground Truth Database. *Pattern Recognition Letters*, 30(2):88-97, 2009.
- [14] L.-C. Chen, G. Papandreou, F. Schroff, and H. Adam. Rethinking Atrous Convolution for Semantic Image Segmentation. *arXiv preprint arXiv:1706.05587*, 2017.
- [15] Y. Yue, W. Zhou, J. Lei, and L. Yu. RTLNet: Recursive Triple-Path Learning Network for Scene Parsing of RGB-D Images. *IEEE Signal Processing Letters*, 29:429-433, 2022.
- [16] W. Zhou, S. Lv, J. Lei, T. Luo, and L. Yu. RFNet: Reverse Fusion Network with Attention Mechanism for RGB-D Indoor Scene Understanding. *IEEE Transactions on Emerging Topics in Computational Intelligence*, 7(2):598-603, 2023.
- [17] V. Badrinarayanan, A. Kendall, and R. Cipolla. SegNet: A Deep Convolutional Encoder-Decoder Architecture for Image Segmentation. *IEEE Transactions on Pattern Analysis and Machine Intelligence*, 39(12):2481-2495, 2017.
- [18] F. Foroughi, J. Wang, A. Nemati, and Z. Chen. MapSegNet: A Fully Automated Model Based on the Encoder-Decoder Architecture for Indoor Map Segmentation. *IEEE Access*, 9:101530-101542, 2021.
- [19] R. K. Srivastava, K. Greff, J. Schmidhuber. Highway networks. *arXiv preprint arXiv:1505.00387*, 2015.
- [20] H. Yan, C. Zhang, and M. Wu. Lawin Transformer: Improving Semantic Segmentation Transformer with Multi-Scale Representations via Large Window Attention. *arXiv preprints arXiv:2201.01615v1*, 2022.
- [21] K. Li, Z. Wu, K.-C. Peng, J. Ernst, and Y. Fu. Guided Attention Inference Network. *IEEE Transactions on Pattern Analysis and Machine Intelligence*, 42(12):2996-3010, 2020.
- [22] J. Li, S. Zha, C. Chen, M. Ding, T. Zhang, and H. Yu. Attention Guided Global Enhancement and Local Refinement Network for Semantic Segmentation. *IEEE Transactions on Image Processing*, 31:3211-3223, 2022.
- [23] S. Xie, R. Girshick, P. Dollár, Z. Tu, and K. He. Aggregated residual transformations for deep neural networks. In *CVPR*, pages 1492-1500, 2017.
- [24] J. Hu, L. Shen, S. Albanie, G. Sun, and E. Wu. Squeeze-and-Excitation Networks. *IEEE Transactions on Pattern Analysis and Machine Intelligence*, 42(8):2011-2023, 2020.
- [25] M.-H. Guo, Z.-N. Liu, T.-J. Mu, and S.-M. Hu. Beyond Self-attention: External Attention using Two Linear Layers for Visual Tasks. *IEEE Transactions on Pattern Analysis and Machine Intelligence*, 45(5):5436-5447, 2023.
- [26] X. Ding, C. Shen, T. Zeng, and Y. Peng. SAB Net: A Semantic Attention Boosting Framework for Semantic Segmentation. *IEEE Transactions on Neural Networks and Learning Systems*, 2022.
- [27] Z. Li, Y. Sun, L. Zhang, and J. Tang. CTNet: Context-Based Tandem Network for Semantic Segmentation. *IEEE Transactions on Pattern Analysis and Machine Intelligence*, 44(12):9904-9917, 2022.
- [28] Y. Li, T. Yao, Y. Pan, and T. Mei. Contextual Transformer Networks for Visual Recognition. *IEEE Transactions on Pattern Analysis and Machine Intelligence*, 45(2):1489-1500, 2023.
- [29] L. Ye, M. Rochan, Z. Liu, X. Zhang, and Y. Wang. Referring Segmentation in Images and Videos with Cross-Modal Self-Attention Network. *IEEE Transactions on Pattern Analysis and Machine Intelligence*, 44(7):3719-3732, 2022.
- [30] Y. Yang and X. Gu. Joint Correlation and Attention Based Feature Fusion Network for Accurate Visual Tracking. *IEEE Transactions on Image Processing*, 32:1705-1715, 2023.
- [31] S. Sang, Y. Zhou, M. T. Islam, and L. Xing. Small-Object Sensitive Segmentation Using Across Feature Map Attention. *IEEE Transactions on Pattern Analysis and Machine Intelligence*, 45(5):6289-6306, 2023.
- [32] J. Choe, S. Lee, and H. Shim. Attention-Based Dropout Layer for Weakly Supervised Single Object Localization and Semantic Segmentation. *IEEE Transactions on Pattern Analysis and Machine Intelligence*, 43(12):4256-4271, 2021.
- [33] Y. Liu, Y. Chen, P. Lasang, and Q. Sun. Covariance Attention for Semantic Segmentation. *IEEE Transactions on*

- Pattern Analysis and Machine Intelligence*, 44(4):1805-1818, 2022.
- [34] G. Yang, P. Rota, X. Alameda-Pineda, D. Xu, M. Ding, and E. Ricci. Variational Structured Attention Networks for Deep Visual Representation Learning. *IEEE Transactions on Image Processing*.
- [35] S. Hao, Y. Zhou, Y. Guo, R. Hong, J. Cheng, and M. Wang. Real-Time Semantic Segmentation via Spatial-Detail Guided Context Propagation. *IEEE Transactions on Neural Networks and Learning Systems*, 2022.
- [36] J. Cao, H. Leng, D. Lischinski, D. Cohen-Or, C. Tu, and Y. Li. ShapeConv: Shape-aware Convolutional Layer for Indoor RGB-D Semantic Segmentation. In *2021 IEEE/CVF International Conference on Computer Vision (ICCV)*, Montreal, QC, Canada, 2021.
- [37] X. Chen, K.-Y. Lin, J. Wang, W. Wu, C. Qian, H. Li, and G. Zeng. Bi-directional Cross-Modality Feature Propagation with Separation-and-Aggregation Gate for RGB-D Semantic Segmentation. In *ECCV 2020. Lecture Notes in Computer Science*, 2020.
- [38] Y. Jian, Y. Yang, Z. Chen, X. Qing, Y. Zhao, L. He, X. Chen, and A. W. Luo. PointMTL: Multi-Transform Learning for Effective 3D Point Cloud Representations. *IEEE Access*, 9:126241-126255, 2021.
- [39] J. Yang, B. Zou, H. Qiu, and Z. Li. MLFNet- Point Cloud Semantic Segmentation Convolution Network Based on Multi-Scale Feature Fusion. *IEEE Access*, 9:44950-44962, 2021.
- [40] M. Cordts, M. Omran, S. Ramos, T. Rehfeld, M. Enzweiler, R. Benenson, U. Franke, S. Roth, and B. Schiele. The cityscapes dataset for semantic urban scene understanding. In *CVPR*, pages 3213-3223, 2016.
- [41] F. Yu and V. Koltun. Multi-Scale Context Aggregation by Dilated Convolutions. In *International Conference on Learning Representations (ICLR)*, 2016.
- [42] C. Yu, J. Wang, C. Peng, C. Gao, G. Yu, and N. Sang. BiSeNet: Bilateral Segmentation Network for Real-time Semantic Segmentation. In *ECCV*, 2018.
- [43] S. Chandra, C. Couprie, and I. Kokkinos. Deep Spatio-Temporal Random Fields for Efficient Video Segmentation. In *CVPR*, 2018.
- [44] Y. Zhu, K. Sapra, F. A. Reda, K. J. Shih, and S. Newsam. Improving Semantic Segmentation via Video Propagation and Label Relaxation. In *CVPR*, pages 8848-8857, 2019.
- [45] J. Wang, C. Gou, Q. Wu, H. Feng, J. Han, E. Ding, and J. Wang. RTFormer: Efficient Design for Real-Time Semantic Segmentation with Transformer. In *36th Conference on Neural Information Processing Systems (NeurIPS 2022)*, New Orleans, LA, USA, 2022.
- [46] W. Yin, Y. Liu, C. Shen, A. van den Hengel, and B. Sun. The devil is in the labels: Semantic segmentation from sentences. *arXiv preprint arXiv:2202.02002v1*, 2022.
- [47] Y. Zhu, Z. Zhang, C. Wu, Z. Zhang, T. He, H. Zhang, R. Manmatha, M. Li, and A. Smola. Improving Semantic Segmentation via Efficient Self-Training. *IEEE Transactions on Pattern Analysis and Machine Intelligence*.
- [48] H. Zhao, J. Shi, X. Qi, X. Wang, and J. Jia. Pyramid Scene Parsing Network. In *CVPR*, pages 2881-2890, 2017.
- [49] T. Takikawa, D. Acuna, V. Jampani, and S. Fidler. Gated-SCNN: Gated Shape CNNs for Semantic Segmentation. In *2019 IEEE/CVF International Conference on Computer Vision (ICCV)*, Seoul, Korea (South), 2019.
- [50] S. Choi, J. T. Kim, and J. Choo. Cars Can't Fly Up in the Sky: Improving Urban-Scene Segmentation via Height-Driven Attention Networks. In *CVPR*, pages 8848-8857, 2020.
- [51] L.-C. Chen, M. D. Collins, Y. Zhu, G. Papandreou, B. Zoph, F. Schroff, H. Adam, and J. Shlens. Searching for Efficient Multi-Scale Architectures for Dense Image Prediction. In *Advances in Neural Information Processing Systems 31 (NeurIPS 2018)*, 2018.
- [52] B. Cheng, M. D. Collins, Y. Zhu, T. Liu, T. S. Huang, H. Adam, and L.-C. Chen. Panoptic-DeepLab: A Simple, Strong, and Fast Baseline for Bottom-Up Panoptic Segmentation. In *CVPR*, 2020.
- [53] X. Chen, K.-Y. Lin, J. Wang, W. Wu, C. Qian, H. Li, and G. Zeng. Bi-directional Cross-Modality Feature Propagation with Separation-and-Aggregation Gate for RGB-D Semantic Segmentation. *arXiv preprint: 2007.09183v1*, 2020.
- [54] Y. Yuan, X. Chen, and J. Wang. Object-Contextual Representations for Semantic Segmentation. In *Computer Vision—ECCV 2020: 16th European Conference*, Glasgow, UK, 2020.
- [55] A. Tao, K. Sapra, and B. Catanzaro. Hierarchical Multi-Scale Attention for Semantic Segmentation. *arXiv preprints: 2005.10821v1*, 2020.
- [56] H. Zhao, Y. Zhang, S. Liu, J. Shi, C. C. Loy, D. Lin, and J. Jia. PSANet: Point-wise Spatial Attention Network for Scene Parsing. In *ECCV*, 2018.
- [57] Y. Yuan, X. Chen, X. Chen, and J. Wang. Segmentation Transformer: Object-Contextual Representations for Semantic Segmentation. In *ECCV*, 2020.
- [58] H. Zhang, C. Wu, Z. Zhang, Y. Zhu, H. Lin, Z. Zhang, Y. Sun, T. He, J. Mueller, R. Manmatha, M. Li, and A. Smola. ResNeSt: Split-Attention Networks. In *2022 IEEE/CVF Conference on Computer Vision and Pattern Recognition Workshops (CVPRW)*, New Orleans, LA, USA, 2022.
- [59] C. Liu, L.-C. Chen, F. Schroff, H. Adam, W. Hua, A. L. Yuille, and L. Fei-Fei. Auto-DeepLab: Hierarchical Neural Architecture Search for Semantic Image Segmentation. In *CVPR*, pages 82-92, 2019.
- [60] Q. Yu, H. Wang, S. Qiao, M. Collins, Y. Zhu, H. Adam, A. Yuille, and L.-C. Chen. kMaX-DeepLab: k-means Mask Transformer. In *ECCV*, 2022.
- [61] A. Valada, R. Mohan, and W. Burgard. Self-Supervised Model Adaptation for Multimodal Semantic Segmentation. *International Journal of Computer Vision*, 128:1239–1285, 2020.
- [62] R. Mohan and A. Valada. EfficientPS: Efficient Panoptic Segmentation. *International Journal of Computer Vision*, 129:1551–1579, 2021.